Howard Hughes Medical Institute

Published as: *Nat Immunol*. 2014 April ; 15(4): 393–401.

Negative Regulation of *Hif1a* Expression and T_H17 Differentiation by Hypoxia Regulated miR-210

Haopeng Wang[#1], **Henrik Flach**[#1], **Michio Onizawa**[2], **Lai Wei**[3], **Michael T McManus**[4], and **Arthur Weiss**[1]

[1]Departments of Medicine and of Microbiology & Immunology, the Rosalind Russell-Ephraim P. Engleman Medical Research Center for Arthritis, and the Howard Hughes Medical Institute, University of California, San Francisco, CA 94143

[2]Department of Medicine University of California, San Francisco

[3]State Key Laboratory of Ophthalmology, Zhongshan Ophthalmic Center, Sun Yat-sen University, Guangzhou, China.

[4]Diabetes Center, University of California, San Francisco

[#] These authors contributed equally to this work.

Abstract

MicroRNA-210 (miR-210) is a signature microRNA of hypoxia. We found robust increase (>100-fold) of miR-210 abundance in activated T cells, especially in the T_H17 lineage. Hypoxia synergized with T cell receptor (TCR)–CD28 stimulation to accelerate and increase the magnitude of *Mir210* expression. *Mir210* was directly regulated by HIF-1α, a key regulator of T_H17 polarization. Surprisingly, *Hif1a* was identified as a miR-210-target, suggesting negative-feedback by miR-210 to inhibit HIF-1α protein expression. Deletion of *Mir210* promoted T_H17 differentiation under conditions with limited oxygen. In experimental colitis, miR-210 reduced *Hif1a* transcript abundance, reduced the proportion of cells producing inflammatory cytokines and controlled disease severity. Our study identifies miR-210 as an important regulator of T cell differentiation in hypoxia, which can limit immunopathology.

Introduction

We usually study *in vitro* T cell responses at the atmospheric O_2 concentration of 21%. However, oxygen tensions in lymphoid tissues are markedly lower (<5%) than those found in peripheral arterial blood (13%)[1, 2]. Immune cells are exposed to varying oxygen tensions

Correspondence should be addressed to A. W. (aweiss@medicine.ucsf.edu).

AUTHOR CONTRIBUTIONS

H.W. and H.F. planned and conducted experiments, analyzed and interpreted data and wrote the manuscript. M.O. performed histology analysis. L.W. contributed critical pre-publication data. M.T.M. provided guidance and direction and the *Mir210* targeted mice. A.W. supervised the work, helped conceive the experiments, and edited the manuscript.

COMPETING INTERESTS STATEMENT

The authors declare that they have no competing financial interests.

in lymphoid organs[2]. T cells are activated during antigen recognition at inflammatory or tumor sites, both of which are hypoxic[2]. Moreover, hypoxic extracellular environments exist in healthy and diseased non-lymphoid tissues, including adipose tissue[3], skin[4] and the gastrointestinal tract[5]. Therefore, activated T cells are dependent on an intracellular machinery that enables them to adapt to changes in oxygen tension and execute their functions *in situ*. The transcription factor hypoxia-inducible factor 1 (HIF-1), mediates at least some of the required metabolic switches from oxidative phosphorylation to aerobic glycolysis in response to hypoxia[6].

The HIF-1 complex consists of two subunits, HIF-1α and HIF-1β[7]. Under normoxic conditions, HIF-1α is proline hydroxylated by prolyl hydroxylases (PHDs) that promotes its binding to the von Hippel Lindau protein (VHL) E3 ligase complex, followed by HIF-1α ubiquitination and proteasomal degradation[8, 9]. Hypoxic conditions inhibit HIF-1α degradation and lead to its stabilization. Recently, a further regulatory layer in non-lymphocytes was described, revealing that in intestinal epithelial cells *Hif1a* is negatively regulated by microRNA-155 (miR-155) during prolonged hypoxia[10].

In addition to the cellular response to hypoxia, HIF-1 plays an important role in regulating T_H17 differentiation. T_H17 cells mount responses against extracellular bacterial and fungal infections in the intestine and the airways[11]. Despite the benefit of such immune responses, T_H17 cells can also play immunopathologic roles in experimental as well as naturally occurring autoimmune settings, including collagen-induced arthritis, experimental autoimmune encephalomyelitis (EAE) or inflammatory bowel diseases (IBD)[12-14]. HIF-1 promotes T_H17 differentiation by directly inducing *Rorc* transcription and subsequently collaborates with RORγt to regulate downstream T_H17 genes and inhibiting regulatory T cell (T_{reg}) differentiation through an active process that targets Foxp3 protein for degradation[15]. In addition, deficiency of *Hif1a* in T cells diminishes the expression of glycolytic molecules and alters the dichotomy between these two T cell subsets, demonstrating that HIF-1α induces metabolic reprogramming and orchestrates lineage differentiation of T cells[16].

miRNAs are noncoding single-stranded RNAs of about 22 nucleotides that mediate sequence-dependent posttranscriptional negative regulation of gene expression[17]. Various stresses, including hypoxia, regulate miRNA expression and function[18]. For example, a subset of miRNAs induced by hypoxia, referred to as “hypoxamiRs”, contribute to the regulation of the broad spectrum of genes regulated by hypoxia. Among these miRNAs, miR-210 is the master hypoxamiR and regulates a variety of cellular events in non-lymphoid tissues[19-22].

Recent work has identified miRNAs as pivotal regulators of helper T cell differentiation and function[23, 24]. Two genome-wide miRNA-profiling studies in activated T cells revealed that miR-210 is highly expressed after T cell stimulation[25, 26]. However, *Mir210*-regulation and its role in T cell activation and differentiation have not been studied.

Results

T cell activation robustly induces *Mir210*

Two independent studies of global miRNA expression profiling in lymphocytes reported that miR-210 is highly expressed in activated mouse T cells (**Supplementary Fig. 1**)[25, 26]. To address the miR-210 expression pattern in more detail, we assessed the expression of miR-210 during T cell activation by real-time PCR (RT-PCR) following the stimulation of naive mouse $CD4^+$ T cells with anti-CD3 and anti-CD28. TCR-CD28 stimulation led to an over 500-fold increase in miR-210 abundance in $CD4^+$ T cells that were activated for 4 d compared to unstimulated cells (**Fig. 1a**). In contrast to interleukin 2 (*Il2*), which was rapidly upregulated by 12 h post stimulation, miR-210 abundance increased more slowly and reached highest amounts at 4 d after T cell activation, suggesting a possible regulatory role of miR-210 in later stages of T cell activation and function (**Fig. 1a,d**). We tested whether induction of *Mir210* also occurs *in vivo* in activated $CD4^+$ T cells using two different approaches. First, we examined miR-210 expression in homeostatically expanded $CD4^+$ T cells isolated from various lymphoid tissues. To this end, naive $CD4^+$ T cells were sorted and adoptively transferred into congenic *Rag2*$^{-/-}$ mice. After 3 weeks, we harvested cells from the spleen, inguinal lymph nodes (ILNs), mesenteric lymph nodes (MLNs), lung and small intestine. After their homeostatic expansion, the transferred $CD4^+$ T cells isolated from the different tissues displayed a uniform, memory-like ($CD44^{hi}$ $CD62L^-$) phenotype and all of the samples moderately upregulated miR-155, an antigen stimulation-induced microRNA[27] (**Fig. 1b** and **Supplementary Fig. 2a**). miR-210 was also upregulated in these T cells, but unlike miR-155, miR-210 showed a distinct expression pattern, with much higher expression in $CD4^+$ T cells isolated from hypoxic tissues like the small intestine, compared to $CD4^+$ T cells isolated from relatively normoxic tissues like the lung. This suggests that miR-210 might play a more critical role in T cells residing within hypoxic sites. We also tested the *in vivo* induction of *Mir210* following ovalbumin (OVA) immunization. We transferred naive $CD4^+$ T cells isolated from OT-II TCR-transgenic mice (specific for the OVA-peptide 323–339) into congenic recipient mice, followed by OVA challenge. Compared to naive T cells, miR-210 was markedly upregulated in these T cells (**Fig. 1c**). Similarly, *Mir210* was robustly induced during $CD8^+$ T cell activation both by *in vitro* stimulation and by using a mouse model of lymphocytic choriomeningitis virus (LCMV) infection (**Supplementary Fig. 2b,c**). Collectively, these data suggest that T cell activation leads to markedly increased miR-210 expression both *in vitro* and *in vivo*.

To study how *Mir210* is regulated during T cell differentiation, naive $CD4^+$ T cells were *in vitro* polarized into T_H1, T_H2, T_H17 and T_{reg} cells and the time-dependent appearance of miR-210 was measured during the process of polarization. The highest increase in miR-210 was observed in T_H17 cells, suggesting a preferential role of miR-210 in T_H17 polarization or function (**Fig. 1d**).

CD28– but not IL-2–signaling controls *Mir210* expression

To examine whether CD28-mediated costimulation is involved in the upregulation of *Mir210*, we stimulated naive $CD4^+$ T cells using anti-CD3 in the absence or presence of anti-CD28. miR-210 abundance in samples costimulated with anti-CD28 was 6-fold higher

than in samples that were stimulated with anti-CD3 alone (**Fig. 2a**). Since CD28 costimulation is known to promote IL-2 production[28] and the induction of *Il2* transcripts preceded the induction of *Mir210* (**Fig. 1a**), we investigated whether CD28-mediated costimulation might indirectly induce *Mir210* by assessing miR-210 abundance in IL-2–deficient, $CD4^+$ T cells (**Fig. 2b**). Whereas the expression of the IL-2-regulated miR-182 in IL-2–deficient $CD4^+$ T cells was markedly reduced following TCR stimulation (**Fig. 2b** top)[29], IL-2–deficiency had no effect on miR-210 expression, suggesting that IL-2 signaling is not required for the induction of *Mir210* (**Fig. 2b** bottom).

Since phosphatidylinositol-3-OH kinase (PI(3)K) signaling is a major CD28 downstream signaling pathway[30], we addressed the requirement of PI(3)K for the induction of *Mir210* with small molecule inhibitors of enzymes involved in the PI(3)K signaling pathways. Whereas CP550690, an inhibitor of Jak1 and Jak3, showed no inhibitory effect on the expression of miR-210 in TCR–CD28-stimulated T cells, both PI(3)K (LY294002 and GDC-0941) and mTOR (rapamycin and MLN0128) inhibitors potently suppressed miR-210 expression (**Fig. 2c**). Thus, the induction of *Mir210* in activated T cells is dependent upon the PI(3)K–mTOR pathway.

HIF-1α is required for *Mir210* induction

To study the influence of hypoxia on the regulation of *Mir210* in T lymphocytes, we compared the induction of *Mir210* in resting versus anti-CD3 and anti-CD28 stimulated primary $CD4^+$ T cells under normoxic (21% O_2) or hypoxic (1% O_2) conditions. TCR stimulation under normoxia resulted in a robust but delayed upregulation of miR-210 (**Fig. 3a**). Unstimulated, T cells increased miR-210 abundance only modestly under hypoxic conditions, suggesting that in T cells, unlike other cell types, hypoxia alone is insufficient to induce robust miR-210 expression. However, stimulated $CD4^+$ and $CD8^+$ T cells exhibited rapid and markedly increased expression of miR-210 in hypoxia, suggesting a synergistic effect of TCR-stimulation and hypoxia (**Fig. 3a** and **Supplementary Fig. 2b**). Notably, this observation was specific for miR-210 since the abundance of miR-155 was not affected by oxygen tension during T cell activation (**Supplementary Fig. 2d**).

Since HIF-1α is the master regulator of hypoxic gene expression, we reasoned that HIF-1α might regulate *Mir210* in T lymphocytes, as shown for other cell types[31]. Therefore, we compared HIF-1α protein abundance in resting versus TCR-stimulated $CD4^+$ T cells under normoxic or hypoxic conditions. TCR-stimulation under both settings resulted in the accumulation of HIF-1α protein by 24 h (**Fig. 3b,c**). Consistent with miR-210 expression, hypoxia also led to more HIF-1α protein than in normoxia on day 1. Similar results were also found after $CD8^+$ T cell activation (**Supplementary Fig. 3a**). The observations that both miR-210 and HIF-1α expression were regulated by oxygen tension and that the expression of HIF-1α preceded the induction of *Mir210* support the notion that HIF-1 acts upstream of miR-210. Furthermore, we found that CD28– deficiency resulted in substantial reductions of HIF-1α protein in activated T cells (**Supplementary Fig. 3b**), indicating that TCR-CD28 signaling may induce *Mir210* via HIF-1α.

To test this hypothesis, we studied TCR signaling-induced *Mir210* expression under normoxic conditions in the presence or absence of HIF-1α. Whereas in HIF-1α–sufficient T cells anti-CD3–anti-CD28 stimulation resulted in robust upregulation of both *Hif1a* transcripts and miR-210, the induction of *Mir210* was markedly attenuated in a HIF-1α–deficient background (**Fig. 3d** left and middle), indicating that HIF-1α is required for *Mir210* induction in activated T cells. The deficiency of HIF-1α did not affect global activation of $CD4^+$ T cells since miR-182 expression was largely unaffected by deletion of *Hif1a* (**Fig. 3d** right). Consequently, we reanalyzed a ChIP-seq dataset, performed in a recent study[32] with T_H17 polarized cells, which revealed that after T cell activation HIF-1α directly bound the promoter region of *Mir210*, with a binding peak at about 400 bp upstream of the *Mir210* sequence (**Supplementary Fig. 3c**), thereby demonstrating that *Mir210* is a direct downstream target of HIF-1α in activated T_H17 cells.

Whereas HIF-1α protein abundance was sustained until 2 d post stimulation in normoxia, HIF-1α protein amounts markedly decreased between d 1 and d 2 under hypoxic conditions (**Fig. 3b,c**). Under normoxic conditions, the decrease in HIF-1α protein was detected later, between d 2 and d 3 after TCR stimulation. In both cases, the decrease in HIF-1α protein correlated with increases in miR-210 abundance, raising the possibility that HIF-1α could be both an upstream *Mir210* regulator and a miR-210 target (**Fig. 3b,c**). Similar results were observed in $CD8^+$ T cells activated under normoxic or hypoxic conditions (**Supplementary Fig. 2b, 3a**).

T cell-specific deletion of *Mir210*

To investigate the role of miR-210 in T cells, mice with *lox*P-flanked *Mir210* alleles ($Mir210^{f/f}$)[33] were crossed with CD4-Cre transgenic mice to delete the floxed *Mir210* alleles in T cells (hereafter referred to as $Mir210^{-/-}$ mice). RT-PCR analysis indicated efficient deletion (>98%) of *Mir210* in activated T cells (**Supplementary Fig. 4a**). Consistent with low miR-210 abundance in immature thymocytes (**Supplementary Fig. 4a**), miR-210–deficiency had little effect on T cell development (**Fig. 4a**). Moreover, wild-type and $Mir210^{-/-}$ mice had comparable numbers and distributions of $CD4^+$ and $CD8^+$ T cells in the periphery and the expression of CD62L and CD44 on peripheral $CD4^+$ T cells was unaffected by deletion of *Mir210* in 6-8 week old mice (**Fig. 4b** and data not shown). The development of natural regulatory T cells in the periphery appeared to be unaltered (**Fig. 4b**). T cell proliferation in response to TCR–CD28 or PMA–ionomycin stimulation was also comparable in wild-type or $Mir210^{-/-}$ T cells (**Fig. 4c**). Therefore, miR-210 is not required for T cell development, homeostasis and proliferation.

Hif1a is a miR-210 target gene

To explore the role of miR-210 in T cell differentiation, we used an *in silico* analysis to identify potential target genes of miR-210. We identified miR-210 potential target genes in mouse T cells by performing the following two-step selection process. First, we used four algorithms, Target scan, PicTar, miRDB and miRanda[34-37], to predict miR-210 target genes. All targets predicted by miRanda were scored for an empirical probability of target inhibition using mirSVR scores[38]and a stringent mirSVR score cutoff of -1.1. We combined this list with previously reported miR-210 targets, resulting in 69 potential miR-210 target

genes (**Supplementary Fig. 4b and Supplementary Table 1**). Next, we selected for T cell-expressed target genes according to the Immgen data-base (www.immgen.org), resulting in 21 genes (**Supplementary Fig. 4b and Supplementary Table 1**). We compared their expression by RT-PCR in wild-type or *Mir210*$^{-/-}$ CD4^{+} T cells, which were activated for 4 d. Assuming that miR-210–deficiency resulted in a higher expression of direct miR-210 targets, we identified five candidate genes that exhibited more than two-fold increased expression in *Mir210*$^{-/-}$ CD4^{+} T cells (**Fig. 5a and Supplementary Fig. 4b**). Two of these genes, *Iscu* and *Ndufa4*, were previously reported as miR-210 targets[31, 39, 40]. Surprisingly, *Hif1a*, was the highest upregulated (>4 fold) miR-210 target gene (**Fig. 5a**). To validate this observation, we compared HIF-1α protein in resting and TCR-stimulated wild-type or *Mir210*$^{-/-}$ CD4^{+} T cells under normoxic or hypoxic conditions. Under hypoxia, we detected a marked and sustained increase in HIF-1α protein abundance in activated *Mir210*$^{-/-}$ T cells (**Fig. 5b**). Moreover, a moderate increase in HIF-1α protein was even detected in *Mir210*$^{-/-}$ T cells activated for 3 or 4 d in normoxia (**Fig. 5b**). These results support the notion that *Hif1a* is a miR-210 target gene, and that miR-210 adds an additional layer of regulation by curbing HIF-1α activity under hypoxia. The different kinetics of HIF-1α protein accumulation and degradation in stimulated wild-type CD4^{+} T cells under normoxia or hypoxia (**Fig. 3b, 3c**), likely accounts for the fact that wild-type cells activated for 2 d under hypoxia had slightly lower HIF-1α protein abundance than cells activated under normoxia (**Fig. 5b**). We determined whether ectopic expression of miR-210 decreased *Hif1a* transcript abundance. We reconstituted miR-210 expression in TCR-CD28–activated *Mir210*$^{-/-}$ CD4^{+} T cells by transduction with bicistronic retroviruses expressing GFP and wild-type pri-miR-210 or GFP and a pri-miR-210 variant whose seed region was replaced by a scrambled control sequence (**Fig. 5c**). We sorted GFP^{+} CD4^{+} T cells and found that *Hif1a* expression was markedly decreased by wild-type but not mutant miR-210 (**Fig. 5d**).

Hif1a contains a non-canonical miR-210 targeting site in its 3′ UTR, containing one G:U wobble at position 7 of the 6-mer seed region. Recent HITS-CLIP studies revealed that a sizeable fraction of miRNA binding sites do not obey the seed pairing rule suggesting that non-canonical sites are widespread[41, 42]. One of these studies also provides a T cell-specific genome-wide argonaute (AGO) binding data set (CLIP Base), which enables analysis of target interactions with all miRNAs expressed in activated T cells[42]. CLIP Base shows a large peak of AGO binding to the *Hif1a* 3′ UTR at around 150 bp from the beginning of the 3′ UTR where the predicted miR-210 target site is located (**Supplementary Fig. 5a**). This potential miR-210 target site is highly conserved among multiple species, stressing its evolutionary importance (**Supplementary Fig. 5b**). To determine whether miR-210 binds this site directly, we cloned the full-length *Hif1a* 3′ UTR (>1800 nucleotides) into a luciferase reporter construct, and cotransfected this reporter with miR-210 mimics into *Mir210*$^{-/-}$ CD4^{+} T cells. A control luciferase reporter with a tandem stretch of four perfect miR-210 binding sites (miR-210 sensor) exhibited markedly reduced luciferase activity of the miR-210 sensor, indicating the miR-210 mimics do function *in vivo*. Interestingly, miR-210 expression also suppressed by about 30% the cotransfected *Hif1a* 3′ UTR reporter that contains only a single copy of the putative miR-210 binding (**Fig. 5e**). Importantly, this suppression of *Hif1a* 3′ UTR by miR-210 was abolished by mutation of the miR-210 binding site. Thus, *Hif1a* is a *bona fide* target gene of miR-210.

miR-210 regulates T_H17 polarization under reoxygenation

Since HIF-1 promotes T_H17 differentiation[15, 16], we investigated the potential role of miR-210 in T_H17 cell differentiation *in vitro*. We compared the efficiency of wild-type or *Mir210*$^{-/-}$ naive T cells to differentiate into T_H17 cells in normoxia or an oxygen-limited environment. Under hypoxic conditions (1% O_2), the expansion of activated T cells was severely impaired (**Supplementary Fig. 5c**). Therefore, reoxygenation conditions have been used to study T_H17 cell differentiation[43]. Reoxygenation has been used to reflect the changes of O_2 concentration experienced by migrating T cells *in vivo* and involves the differentiation of T_H17 cells by a priming step under a low O_2 concentration (5% O_2) followed by transfer to normoxic conditions[43] (**Supplementary Fig. 6a**). T_H17 differentiation was promoted under reoxygenation versus normoxia under suboptimal (0.2 ng/ml IL-6), intermediate (2.0 ng/ml IL-6) or maximal (20.0 ng/ml IL-6) T_H17 skewing conditions (**Fig. 6a**). We used suboptimal IL-6 concentration (0.2 ng/ml) in subsequent analyses, since it showed the largest net increase in T_H17 differentiation. Monitoring HIF-1α protein in T_H17 cells polarized under normoxia or reoxygenation, we detected more HIF-1α protein in cells that were activated for 1 d under reoxygenation conditions, and a moderate increase in HIF-1α protein in cells polarized for 1, 2 or 3 d in normoxia (**Fig. 6b**), suggesting a critical role for HIF-1α in T_H17 differentiation in normoxia and reoxygenation conditions[15, 16, 43]. Consequently, $CD4^+$ T cells polarized under reoxygenation conditions exhibited a more rapid and increased expression of miR-210 (**Fig. 6c**), which was associated with a rapid decrease in HIF-1α protein between d 1 and d 2 (**Fig. 6b, 6c**). Similar results were observed in activated T cells in nonpolarizing conditions (**Supplementary Figure 6b,c**). Notably, the increase of T_H17 differentiation under reoxygenation, compared to normoxia, was reduced by about 50% in *Hif1a*$^{f/+}$ CD4-Cre and was abolished in *Hif1a*$^{f/f}$ CD4-Cre T cells, indicating that HIF-1α protein is limiting for the differentiation of T_H17 cells under reoxygenation conditions (**Fig. 6d**).

Whereas deficiency in miR-210 had subtle effects on T_H17 differentiation under normoxic conditions, *Mir210* deletion markedly increased the proportion of T_H17 cells under reoxygenation, especially if low or intermediate IL-6 concentrations were used (**Fig. 7a,b**). By comparing wild-type or *Mir210*$^{-/-}$ $CD4^+$ T cells which were T_H17 polarized under reoxygenation conditions, we observed that *Hif1a* transcript and HIF-1α protein amounts were increased in *Mir210*$^{-/-}$ cells (**Fig. 7c,d**). The increased HIF-1α protein was associated with marked up-regulation of genes encoding key regulators of the glycolytic pathway (**Fig. 7e**), promoting T_H17 differentiation[16]. This correlated well with increased expression of T_H17 signature genes, including *Il17a*, *Il17f*, *Rorc* and *Il23r* (**Fig. 7f**). Intriguingly, the observed increase in lineage differentiation under reoxygenation conditions, and the further polarization by deletion of *Mir210* exclusively applied for the T_H17 subset (**Supplementary Fig. 6d,e**). Next, we investigated intracellular Foxp3 abundance in T_H17-polarized wild-type or *Mir210*$^{-/-}$ $CD4^+$ T cells, skewed under suboptimal (0.2 ng/ml IL-6) T_H17 conditions in normoxia or reoxygenation conditions. Normoxia-cultured cells exhibited a high proportion of $Foxp3^+$ cells, irrespective whether they were miR-210–sufficient or –deficient (**Supplementary Fig. 6f**), consistent with reduced T_H17 differentiation under those conditions (**Fig. 6a**). In contrast, wild-type $CD4^+$ T cells, skewed under reoxygenation conditions exhibited a decreased proportion of $Foxp3^+$ cells (**Supplementary Figure 6f**),

correlating well with increased T_H17 differentiation potential (**Fig. 6a**) and higher HIF-1α protein amounts (**Fig. 6b**). *Mir210* deletion, which resulted in further increase of HIF-1α protein expression under reoxygenation (**Fig. 7d**), caused a further drop of $Foxp3^+$ cells (**Supplementary Fig. 6f**).

To substantiate the model that miR-210 attenuates T_H17 differentiation by targeting *Hif1a*, we generated *Mir210*$^{-/-}$*Hif1a*$^{f/+}$mice, and compared the T_H17 polarization potential of their naive T cells in normoxia or under reoxygenation to naive T cells of wild-type or *Mir210*$^{-/-}$ mice (**Fig. 7a**). Corroborating our previous results, the enhanced T_H17 cell differentiation under reoxygenation caused by miR-210–deficiency was considerably suppressed in *Mir210*$^{-/-}$ *Hif1a*$^{f/+}$ T cells, indicating that miR-210 regulates T_H17 polarization mainly by targeting *Hif1a*.

miR-210 controls IBD severity

The gut is a hypoxic environment[5] and contains a high proportion of IL-17A-producing cells[15]. To test whether miR-210 influences the differentiation of T_H17 cells during an inflammatory bowel disease (IBD) model of colitis, we transferred naive, T_{reg}-depleted ($CD45.2^+$) T cells from wild-type or *Mir210*$^{-/-}$ mice into $CD45.1^+$ *Rag2*$^{-/-}$ mice. Five weeks after T cell transfer, wild-type T cells from the lamina propria contained a marked increase in miR-210 abundance compared to naive T cells (**Fig. 8a**). Consistent with the reoxygenation *in vitro* model, miR-210–deficiency *in vivo* resulted in a markedly increased transcript and protein expression of HIF-1α in *Mir210*$^{-/-}$ intestinal T cells (**Fig. 8a,b**). In contrast, splenic T cells isolated from the same animals did not upregulate HIF-1α protein (**Fig. 8b**). Both groups, the $CD45.2^+$ wild-type T cell-transferred control and the $CD45.2^+$ *Mir210*$^{-/-}$ T cell-transferred group, started to lose body weight about 3-4 weeks after T cell transfer. However, mice reconstituted with *Mir210*$^{-/-}$ T cells exhibited substantially more weight loss, associated with increased mucosal leukocyte infiltration (**Fig. 8c,d**). Moreover, the *Mir210*$^{-/-}$ T cell-transferred group had higher weight/length ratios of the colon, which correlated with worse histopathological scores (**Fig. 8e**), evidence of more severe disease in the absence of miR-210. We measured the percentages of IL-17A-producing cells among $CD4^+$ T cells, isolated from the lamina propria of the sick animals and observed a marked increase in the proportion of $IL\text{-}17A^+$ T cells in *Mir210*$^{-/-}$ T cell-transferred mice, indicating that miR-210 controls T_H17 differentiation *in vivo* (**Fig. 8f**). Furthermore, the proportion of $IL\text{-}17A^+$ interferon-γ (IFN-γ^+) double-positive cells and IFN-γ^+ single-positive cells were increased, indicating that miR-210–deficiency may also facilitate the conversion of T_H1-like cells from T_H17 cells (**Fig. 8f**). Collectively, these results support an important role for miR-210 in controlling T_H17 T cell differentiation and the development of immunopathology *in vivo*.

Discussion

In two independent global microRNA expression profiling studies in lymphocytes, miR-210 was shown to be induced in effector T cells[25, 26]. Our studies support and extend these findings by suggesting miR-210 plays a particularly important role in regulating the T_H17 T cell lineage. We found that TCR stimulation led to a robust induction of *Mir210* in T cells

under normoxic conditions. Moreover, hypoxia-challenged and antigen-stimulated T cells exhibited a more rapid and increased induction of *Mir210*, suggesting that multiple signals are required for optimal *Mir210* induction. Signals provided by antigen and costimulatory stimulation synergize with signals provided by the hypoxic environment. Immune cells encounter rapid changes in oxygen tension as they develop and migrate into different compartments of the body[44]. Therefore, a hypoxia-mediated signal to properly induce *Mir210* is an intriguing and additional layer of regulation for microRNAs critical in the immune system. *Mir210* is only fully induced when T cells are activated at inflammatory sites or in cancerous tissues, both of which are considered hypoxic[45]. What might be a possible biological function of this HIF-1α-induced microRNA under hypoxic conditions? miR-210 is not only upregulated by HIF-1α, but also negatively regulates *Hif1a* transcript and HIF-1α protein abundance in peripheral T cells, providing the first example of desensitizing HIF-1 activity by a microRNA in lymphocytes under hypoxic conditions.

In contrast to normoxia, hypoxic conditions inhibit HIF-1α degradation and lead to its stabilization[8, 9]. However, the mechanism by which HIF-1α activity is turned off to prevent its excessive activation in hypoxia was obscure. Two principal mechanisms have been proposed. First, although the hydroxylation activity of PHD is limited in hypoxia, the HIF-1α-driven increased expression of PHD2 and PHD3 under hypoxic conditions may compensate for the loss of their activities and consequently represents a negative-feedback loop targeting HIF-1α expression at the protein level[46-48]. Second, hypoxia-induced miR-155 directly targets *Hif1a* in intestinal epithelial cells, desensitizing HIF-1 activity at the transcript level[10]. However, we found that miR-155 is not a hypoxia-regulated microRNA in human or mouse T cells and suggest that the “hypoxamiR” miR-210 acts to specifically negatively regulate HIF-1α activity in T cells at later stages of activation.

Priming of naive T cells under O_2-limiting (5%) conditions, significantly increases HIF-1α protein and thereby accelerates T_H17 differentiation[43]. T cell-specific deletion of VHL, results in more HIF-1α and further increases T_H17 differentiation under reoxygenation conditions[43]. We showed that HIF-1α-induced *Mir210* is highly expressed in T_H17 cells and that miR-210 directly suppresses *Hif1a* transcript abundance. Therefore, miR-210 appears to play a role in feedback inhibition to curb HIF-1 activity in T cells under hypoxia and consequently restraining T_H17 cell differentiation and associated immunopathology. This is consistent with less *Hif1a* in response to ectopic expression of miR-210 and a marked upregulation of *Hif1a* mRNA and protein in activated, $Mir210^{-/-}$ T cells. This effect was most evident under reoxygenation conditions *in vitro* and in hypoxic environments *in vivo* suggesting that miR-210 plays its most important tuning role in low-oxygen conditions.

Consistent with many miRNA knockouts exhibiting phenotypes only under stress conditions[49], $Mir210^{-/-}$ T cells revealed enhanced T_H17 polarization under reoxygenation, but not normoxia. Low oxygen tension increases the described HIF-1α–miR-210 regulatory feedback loop in two ways. Firstly, hypoxia synergizes with TCR-CD28 stimulation to prompt more rapid and robust induction of *Mir210*, which secondly leads to a more profound negative regulation of *Hif1a* mRNA, resulting in curbed HIF-1α activity in hypoxia. Therefore, miR-210 is a crucial regulator of HIF-1 activity and T_H17 differentiation in low-oxygen conditions, which is further corroborated by our IBD studies.

HIF-1α has been suggested to be a potential therapeutic target for the treatment of a variety of T_H17 cell-mediated autoimmune diseases[15]. Our *in vitro* and *in vivo* studies demonstrate that miR-210 is a potent regulator of *Hif1a* mRNA and protein in T cells under hypoxic conditions. Therefore, targeting *Hif1a* by administrating miR-210 mimics *in vivo* might be an effective therapeutic strategy for T_H17-dependent autoimmune diseases.

Online Methods

Reagents

Rabbit polyclonal antibody against HIF-1α and mouse monoclonal antibody against GAPDH (Abcam, clone 6C5) were purchased from Cayman Chemical and Abcam, respectively. Anti–IL-4 (clone 11B11), anti–IFN-γ (clone XMG1.2), anti-CD3ε (clone 2C11) and anti-CD28 (clone 37.51) were purchased from UCSF Cell Culture Facility. CP550 690 was a gift from J.J. O'Shea (NIH). GDC-0941 and MLN0128 were gifts from K. Shokat (UCSF). LY294002 and Rapamycin were purchased from Millipore. PMA and ionomycin were purchased from Sigma-Aldrich.

Mice

The *Mir210* conditional knockout mice have been generated as described previously[33]. Briefly, $Mir210^{f/f}$ mice were generated by crossing miR-210 (lacZ-neo^r-flox) mice[33] with the actin-Flp deleter mouse strain (Jax) to delete the lacZ–neomycin-resistance cassette, followed by backcrossing to the C57BL/6 (Jax) background for more than 9 generations. The C57BL/6 (Jax), $Cd28^{-/-}$ (Jax), BoyJ (Taconic), $CD45.1^+CD45.2^-Rag2^{-/-}$ (Taconic), CD4-Cre (Taconic), OTII (Taconic) and P14 TCR transgenic (Jax) mouse strains were purchased from the indicated vendors. $Il2^{-/-}$ D011.10 mice and $Hif1a^{f/f}$ mice have been described previously[50, 51]. All mice were housed and bred in specific-pathogen-free conditions in the Animal Barrier Facility at the University of California, San Francisco. All animal experiments were approved by the Institutional Animal Care and Use Committee of the University of California, San Francisco.

RNA Analysis

For microRNA assays, total RNA was extracted with a mirVana miRNA Isolation Kit (Applied Biosystems) and then reverse transcribed with TaqMan Reverse Transcription reagents (Applied Biosystems). TaqMan miRNA assays were performed in an ABI Quantstudio machine (Applied Biosystems). miRNA assay results were normalized to the abundance of snoRNA202. The expression of each miRNA is presented as the fold change relative to its expression in wild-type naive T cells. For RT-PCR of non-miRNA genes, cDNA was synthesized with Superscript III/II reverse transcription (Invitrogen). The information of all primers is listed in **Supplementary Table 2**.

OVA Immunization and LCMV Infection

For the activation of $CD4^+$ T cells, splenic and lymph node-derived naive T cells ($CD4^+CD62L^{hi}CD44^{lo}CD25^-$) were sorted by flow cytometry from OT-II TCR-transgenic mice. After CFSE labeling, the sorted cells were transferred into congenic recipient mice. 24 h later, the recipients were immunized s.c. with the OVA323-339 peptide (100 μg/mouse

Genscript) in the presence of Complete Freund's Adjuvant (CFA; DIFCO). Mice were sacrificed 7 d after immunization, and activated $CD4^+CFSE^{lo}$ T cells were isolated from the draining LN, followed by RNA isolation for miRNA expression analysis. For the *in vivo* activation of $CD8^+$ T cells, P14 transgenic T cells were transferred into congenic recipient mice. The recipients were infected by lymphocytic choriomeningitis virus (LCMV). Naive (d 0), effector (d 8 post infection) and memory (d 202 post infection) LCMV-specific $CD8^+$ T cells were sorted by flow cytometry, followed by RNA isolation for miRNA expression analysis.

In vitro T Cell Activation and Polarization Assays

Sorted naive T cells ($CD4^+CD62L^{hi}CD44^{lo}CD25^-$) were used for *in vitro* culture in RPMI medium (plus β-mercaptoethanol) supplemented with 10% (vol/vol) FBS, 100 μM HEPES pH 7.5 and antibiotics. T cells were activated with plate-bound 2 μg/ml anti-CD3 (clone 2C11; UCSF Cell Culture Facility) and 2 μg/ml anti-CD28 (clone 37.51 UCSF Cell Culture Facility) for 4 d under conditions with various oxygen concentrations. For T_H17 conditions, 10 μg/ml anti–IL-4, 10 μg/ml anti–IFN-γ, 2 ng/ml TGF-β, and 20, 2 or 0.2 ng/ml IL-6 were added to the cultures, and cells were stimulated for 3 d–5 d. Cells were then harvested and stimulated for a period of 5 h with PMA (50 ng/ml) and ionomycin (1 nM) in the presence of GolgiStop (BD-Biosciences), and the differentiated cells were analyzed by flow cytometry for cytokine production by intracellular staining using a LSRFortessa (BD-Biosciences). For the reoxygenation assay, T cells were firstly primed under a low O_2 concentration (5% O_2) for 36 h, and then the cells were transferred into a normoxic incubator for the rest of the culture.

Primary T cell Transfection, Luciferase Reporter Assays and Retroviral Transduction

The lucifierase reporter assays and T cell transfection of miRNA mimics have been described previously[52]. Briefly, the full-length 3′ UTR of *Hif1a* was cloned into the pMIR-REPORT™ luciferase reporter construct (Invitrogen). Isolated naive $CD4^+$ T cells were stimulated with anti-CD3 and anti-CD28 for 4 d. The activated T cells were cotransfected with reporter constructs and miRNA mimics (Dharmacon) by the Neon electroporation transfection system (Invitrogen) with an optimized version of the manufactures' recommended protocol. Luciferase activity was measured 24 h after transfection with the pMIR-REPORT™ miRNA Expression Reporter Vector System (Invitrogen) and a Mithras LB 940 (Berthold Technologies) platereader. Retroviral transduction was performed as described previously[53].

Adoptive Transfer and Chronic Colitis model

The inflammatory bowel disease model has been described previously[54]. Briefly, 1×10^6 flow-sorted naive T cells ($CD4^+CD25^-CD44^-CD62L^+$) were adoptively transferred i.p. into 8–12 week-old $CD45.1^+CD45.2^-$*Rag2*$^{-/-}$ recipient mice (no specific randomization protocol was used). The body weight of each mouse was monitored after adoptive transfer. After mice were sacrificed, the colonic specimens taken from proximal and middle colons were subjected to histopathological assessment. Tissue samples were fixed in 10% neutral buffered formalin (pH7.0). Paraffin-embedded sections were stained with hematoxylin and

eosin. These sections were analyzed and the severity of the inflammation was scored in a blinded manner. The degree of inflammation in the colon was graded according to a modification of the previously described scoring system[54]. Briefly, for mucosal damage, 0 points were assigned to normal appearance, 1 point to discrete lymphoepithelial lesions, 2 points to diffuse crypt elongation or goblet depletion, or 3 points to extensive crypt elongation, mucosal erosion/ulceration. For cell infiltration, 0 points were assigned for normal or for the presence of occasional leukocytes, 1 point for widely scattered leukocytes or focal aggregates of leukocytes, 2 points for the confluence of leukocytes extending into the submucosa with focal effacement of the muscularis, or 3 points for transmural extension of leukocyte infiltration. For crypt abscess, the assigned points were: 0 for no crypt abscess; 1 point for the presence of rare crypt abscess; or, 2 points for multiple crypt abscesses.

Statistical Analysis

Prism software was used for statistical analysis. Differences between groups were compared by unpaired two-tailed *t*-test. A *P* value of less than 0.05 was considered statistically significant.

Supplementary Material

Refer to Web version on PubMed Central for supplementary material.

ACKNOWLEDGMENTS

The authors thank A. Roque for animal husbandry. We thank R. Locksley and Z. Wang for access and assistance with cell sorting; R. Wang (St Jude Children's Research Hospital) for providing organs from *Hif1a*$^{f/f}$ *Cd4-Cre*$^{+}$ mice; M. Matloubian for providing RNA from LCMV infected mice; A. Abbas for providing *Il2*$^{-/-}$ DO11.10 mice; K. Shokat (UCSF) and J. J. O'shea (US National Institutes of Health) for providing kinase inhibitors; K. Mark Ansel and L. Jeker for critical reading of the manuscript. H.W. is a recipient of an Arthritis Foundation Postdoctoral Fellowship and H.F. is a recipient of a DFG Fellowship. L.W. was supported by the National Basic Research Program of China (2013CB967002). This work was also supported in part by a grant from the Keck Foundation.

REFERENCES

1. Caldwell CC, et al. Differential effects of physiologically relevant hypoxic conditions on T lymphocyte development and effector functions. J. Immunol. 2001; 167:6140–6149. [PubMed: 11714773]
2. McNamee EN, Korns Johnson D, Homann D, Clambey ET. Hypoxia and hypoxia-inducible factors as regulators of T cell development, differentiation, and function. Immunol. Res. 2013; 55:58–70. [PubMed: 22961658]
3. Ye J. Emerging role of adipose tissue hypoxia in obesity and insulin resistance. Int. J. Obes. 2009; 33:54–66.
4. Bedogni B, et al. The hypoxic microenvironment of the skin contributes to Akt-mediated melanocyte transformation. Cancer Cell. 2005; 8:443–454. [PubMed: 16338658]
5. Taylor CT, Colgan SP. Hypoxia and gastrointestinal disease. J. Mol. Med. 2007; 85:1295–1300. [PubMed: 18026919]
6. Semenza GL. Hypoxia-inducible factor 1 (HIF-1) pathway. Sci. STKE. 20072007:cm8. [PubMed: 17925579]
7. Wang GL, Jiang BH, Rue EA, Semenza GL. Hypoxia-inducible factor 1 is a basic-helix-loop-helix-PAS heterodimer regulated by cellular O2 tension. Proc. Natl. Acad. Sci. USA. 1995; 92:5510–5514. [PubMed: 7539918]

8. Maxwell PH, et al. The tumour suppressor protein VHL targets hypoxia-inducible factors for oxygen-dependent proteolysis. Nature. 1999; 399:271–275. [PubMed: 10353251]
9. Jaakkola P, et al. Targeting of HIF-alpha to the von Hippel-Lindau ubiquitylation complex by O2-regulated prolyl hydroxylation. Science. 2001; 292:468–472. [PubMed: 11292861]
10. Bruning U, et al. MicroRNA-155 promotes resolution of hypoxia-inducible factor 1alpha activity during prolonged hypoxia. Mol. Cell. Biol. 2011; 31:4087–4096. [PubMed: 21807897]
11. Korn T, Bettelli E, Oukka M, Kuchroo VK. IL-17 and Th17 Cells. Annu. Rev. Immunol. 2009; 27:485–517. [PubMed: 19132915]
12. Weaver CT, Hatton RD, Mangan PR, Harrington LE. IL-17 family cytokines and the expanding diversity of effector T cell lineages. Annu. Rev. Immunol. 2007; 25:821–852. [PubMed: 17201677]
13. Fife BT, et al. Interactions between PD-1 and PD-L1 promote tolerance by blocking the TCR-induced stop signal. Nat. Immunol. 2009; 10:1185–1192. [PubMed: 19783989]
14. Wu S, et al. A human colonic commensal promotes colon tumorigenesis via activation of T helper type 17 T cell responses. Nat. Med. 2009; 15:1016–1022. [PubMed: 19701202]
15. Dang EV, et al. Control of T(H)17/T(reg) balance by hypoxia-inducible factor 1. Cell. 2011; 146:772–784. [PubMed: 21871655]
16. Shi LZ, et al. HIF1alpha-dependent glycolytic pathway orchestrates a metabolic checkpoint for the differentiation of TH17 and Treg cells. J. Exp. Med. 2011; 208:1367–1376. [PubMed: 21708926]
17. Bartel DP. MicroRNAs: target recognition and regulatory functions. Cell. 2009; 136:215–233. [PubMed: 19167326]
18. Leung AK, Sharp PA. MicroRNA functions in stress responses. Mol. Cell. 2010; 40:205–215. [PubMed: 20965416]
19. Chan YC, Banerjee J, Choi SY, Sen CK. miR-210: the master hypoxamir. Microcirculation. 2012; 19:215–223. [PubMed: 22171547]
20. Camps C, et al. hsa-miR-210 Is induced by hypoxia and is an independent prognostic factor in breast cancer. Clin. Cancer Res. 2008; 14:1340–1348. [PubMed: 18316553]
21. Giannakakis A, et al. miR-210 links hypoxia with cell cycle regulation and is deleted in human epithelial ovarian cancer. Cancer Biol. Ther. 2008; 7:255–264. [PubMed: 18059191]
22. Kulshreshtha R, et al. A microRNA signature of hypoxia. Mol. Cell. Biol. 2007; 27:1859–1867. [PubMed: 17194750]
23. O'Connell RM, Rao DS, Chaudhuri AA, Baltimore D. Physiological and pathological roles for microRNAs in the immune system. Nat. Rev. Immunol. 2010; 10:111–122. [PubMed: 20098459]
24. Baumjohann D, Ansel KM. MicroRNA-mediated regulation of T helper cell differentiation and plasticity. Nat. Rev. Immunol. 2013; 13:666–678. [PubMed: 23907446]
25. Kuchen S, et al. Regulation of microRNA expression and abundance during lymphopoiesis. Immunity. 2010; 32:828–839. [PubMed: 20605486]
26. Chong MM, et al. Canonical and alternate functions of the microRNA biogenesis machinery. Genes Dev. 2010; 24:1951–1960. [PubMed: 20713509]
27. Thai TH, et al. Regulation of the germinal center response by microRNA-155. Science. 2007; 316:604–608. [PubMed: 17463289]
28. Fraser JD, Irving BA, Crabtree GR, Weiss A. Regulation of interleukin-2 gene enhancer activity by the T cell accessory molecule CD28. Science. 1991; 251:313–316. [PubMed: 1846244]
29. Stittrich AB, et al. The microRNA miR-182 is induced by IL-2 and promotes clonal expansion of activated helper T lymphocytes. Nat. Immunol. 2010; 11:1057–1062. [PubMed: 20935646]
30. Kane LP, Andres PG, Howland KC, Abbas AK, Weiss A. Akt provides the CD28 costimulatory signal for up-regulation of IL-2 and IFN-gamma but not TH2 cytokines. Nat. Immunol. 2001; 2:37–44. [PubMed: 11135576]
31. Huang X, et al. Hypoxia-inducible mir-210 regulates normoxic gene expression involved in tumor initiation. Mol. Cell. 2009; 35:856–867. [PubMed: 19782034]
32. Ciofani M, et al. A validated regulatory network for Th17 cell specification. Cell. 2012; 151:289–303. [PubMed: 23021777]

33. Park CY, et al. A resource for the conditional ablation of microRNAs in the mouse. Cell Rep. 2012; 1:385–391. [PubMed: 22570807]
34. Wang X, El Naqa IM. Prediction of both conserved and nonconserved microRNA targets in animals. Bioinformatics. 2008; 24:325–332. [PubMed: 18048393]
35. Krek A, et al. Combinatorial microRNA target predictions. Nat. Genet. 2005; 37:495–500. [PubMed: 15806104]
36. John B, et al. Human MicroRNA targets. PLoS Biol. 2004; 2:e363. [PubMed: 15502875]
37. Lewis BP, Shih IH, Jones-Rhoades MW, Bartel DP, Burge CB. Prediction of mammalian microRNA targets. Cell. 2003; 115:787–798. [PubMed: 14697198]
38. Betel D, Koppal A, Agius P, Sander C, Leslie C. Comprehensive modeling of microRNA targets predicts functional non-conserved and non-canonical sites. Genome Biol. 2010; 11:R90. [PubMed: 20799968]
39. Tsuchiya S, et al. MicroRNA-210 regulates cancer cell proliferation through targeting fibroblast growth factor receptor-like 1 (FGFRL1). J. Biol. Chem. 2011; 286:420–428. [PubMed: 21044961]
40. Favaro E, et al. MicroRNA-210 regulates mitochondrial free radical response to hypoxia and krebs cycle in cancer cells by targeting iron sulfur cluster protein ISCU. PLoS One. 2010; 5:e10345. [PubMed: 20436681]
41. Chi SW, Zang JB, Mele A, Darnell RB. Argonaute HITS-CLIP decodes microRNA-mRNA interaction maps. Nature. 2009; 460:479–486. [PubMed: 19536157]
42. Loeb GB, et al. Transcriptome-wide miR-155 binding map reveals widespread noncanonical microRNA targeting. Mol. Cell. 2012; 48:760–770. [PubMed: 23142080]
43. Ikejiri A, et al. Dynamic regulation of Th17 differentiation by oxygen concentrations. Int. Immunol. 2012; 24:137–146. [PubMed: 22207131]
44. Westermann J, Bode U. Distribution of activated T cells migrating through the body: a matter of life and death. Immunol. Today. 1999; 20:302–306. [PubMed: 10379047]
45. Vaupel P, Thews O, Kelleher DK, Hoeckel M. Current status of knowledge and critical issues in tumor oxygenation. Results from 25 years research in tumor pathophysiology. Adv. Exp. Med. Biol. 1998; 454:591–602. [PubMed: 9889939]
46. Henze AT, et al. Prolyl hydroxylases 2 and 3 act in gliomas as protective negative feedback regulators of hypoxia-inducible factors. Cancer Res. 2010; 70:357–366. [PubMed: 20028863]
47. Minamishima YA, et al. A feedback loop involving the Phd3 prolyl hydroxylase tunes the mammalian hypoxic response in vivo. Mol. Cell. Biol. 2009; 29:5729–5741. [PubMed: 19720742]
48. Stiehl DP, et al. Increased prolyl 4-hydroxylase domain proteins compensate for decreased oxygen levels. Evidence for an autoregulatory oxygen-sensing system. J. Biol. Chem. 2006; 281:23482–23491. [PubMed: 16790428]
49. Park CY, Choi YS, McManus MT. Analysis of microRNA knockouts in mice. Hum. Mol. Genet. 2010; 19:R169–175. [PubMed: 20805106]
50. Wang R, et al. The transcription factor Myc controls metabolic reprogramming upon T lymphocyte activation. Immunity. 2011; 35:871–882. [PubMed: 22195744]
51. Hoyer KK, Kuswanto WF, Gallo E, Abbas AK. Distinct roles of helper T-cell subsets in a systemic autoimmune disease. Blood. 2009; 113:389–395. [PubMed: 18815283]
52. Steiner DF, et al. MicroRNA-29 regulates T-box transcription factors and interferon-gamma production in helper T cells. Immunity. 2011; 35:169–181. [PubMed: 21820330]
53. Wang H, et al. Tonic ubiquitylation controls T-cell receptor:CD3 complex expression during T-cell development. EMBO J. 2010; 29:1285–1298. [PubMed: 20150895]
54. Yamaji O, et al. The development of colitogenic CD4(+) T cells is regulated by IL-7 in collaboration with NK cell function in a murine model of colitis. J. Immunol. 2012; 188:2524–2536. [PubMed: 22331065]

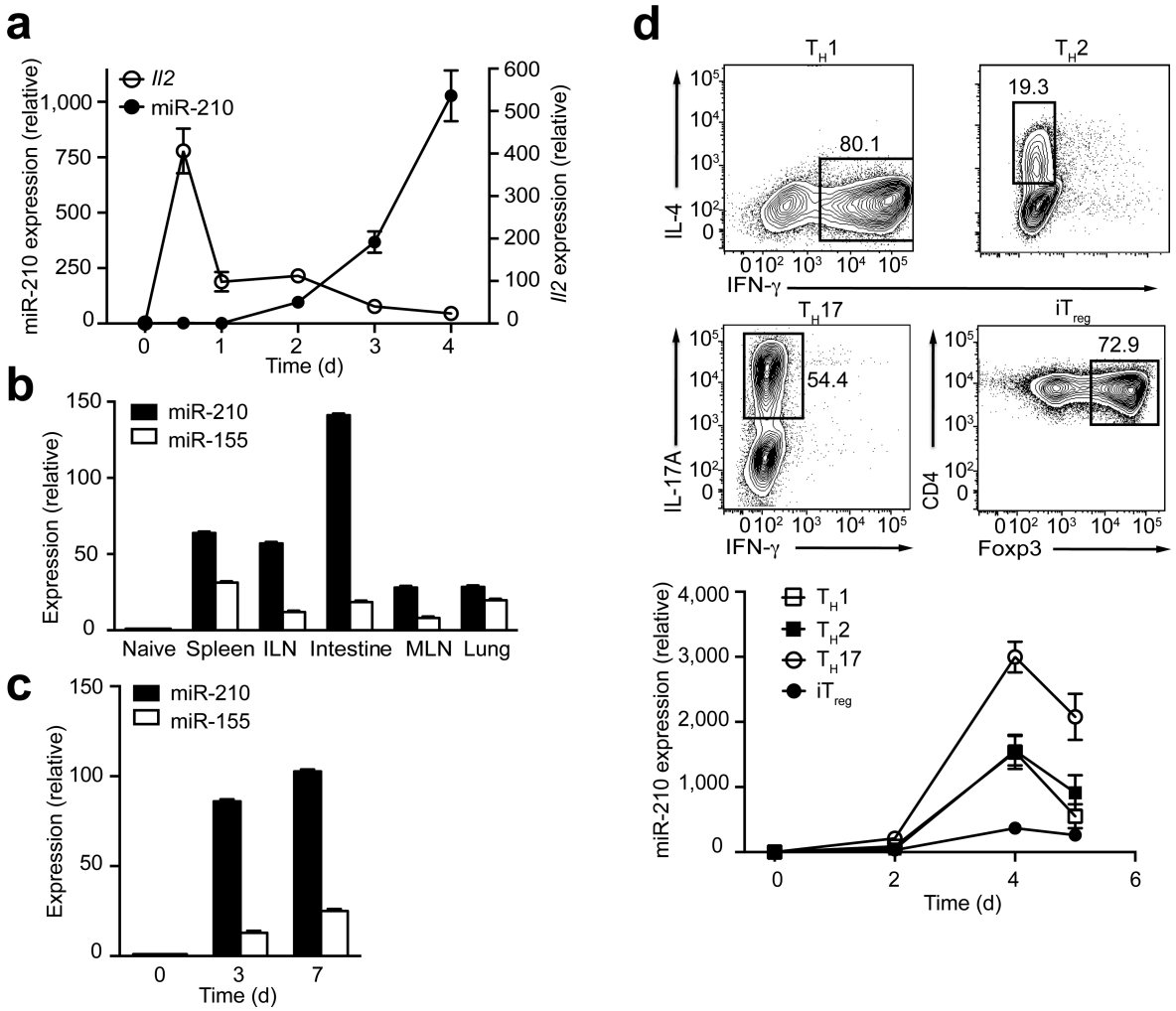

Figure 1.

Mir210 is induced after T cell activation and regulated during T cell differentiation. (**a**) The expression of miR-210 or *Il2* in activated T cells was assessed by RT-PCR. The data were normalized by miR-210 expression in naive T cells (n=3 independent biological replicates per data point). (**b**) Homeostatically expanded $CD4^+$ T cells were sorted from various tissues 3 weeks after adoptive transfer. The expression of miR-210 and miR-155 were assessed by RT-PCR. (**c**) miR-210 and miR-155 expression within *in vivo* activated OTII $CD4^+$ T cells were determined by RT-PCR. (**d**) After 4 d polarizing naive $CD4^+$ T cells towards the T_H1, T_H2, T_H17 or iTreg lineage, cells with selective expression of IFN-γ, IL-4, IL-17A or Foxp3 were assessed by flow cytometry with the percentages of gated cells depicted (top). The time dependency of miR-210 expression in polarized T cells was measured by RT-PCR (bottom). Relative expression is normalized to sno202. Data are from one experiment representative of two (**b**,**c**) or three (**d**) independent experiments (mean and s.d. in **a**–**d**).

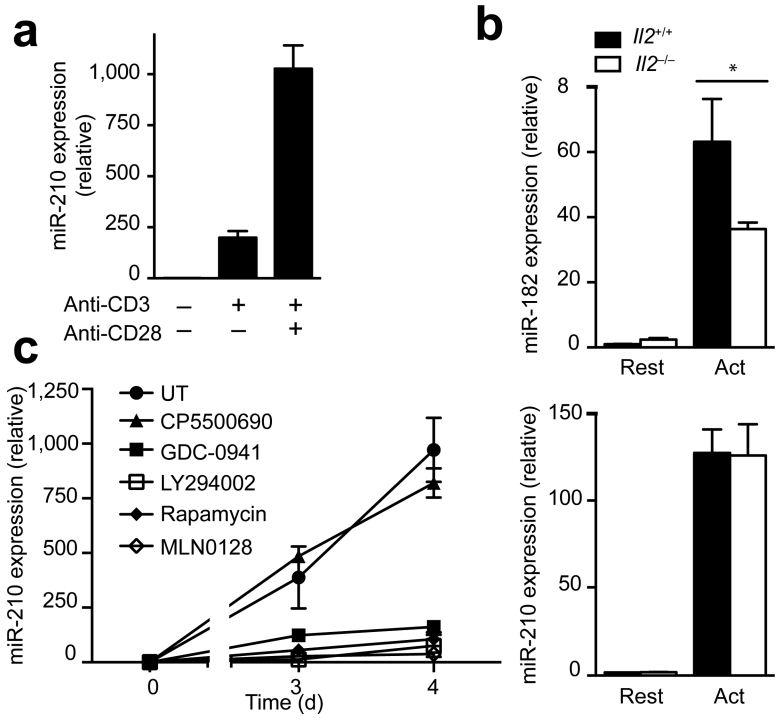

Figure 2.

CD28-costimulation controls *Mir210* expression via the PI(3)K-mTOR pathway. (**a**) Naive $CD4^+$ T cells were activated by anti-CD3 in the presence or absence of anti-CD28 for 4 d and miR-210 expression was analyzed by RT-PCR. (**b**) RT-PCR analysis of miR-182 and miR-210 expression in activated T cells from wild-type or $Il2^{-/-}$ DO11.10 $Rag2^{-/-}$ mice. (**c**) $CD4^+$ naive T cells were stimulated in the presence of the kinase inhibitors CP550 690 (100 nM), GDC-0941 (1 μM), LY294002 (5 μM), Rapamycin (20 nM) or MLN0128 (200 nM). miR-210 expression was measured by RTPCR. Relative expression is normalized to sno202 (n=3 independent biological replicates per data point). Data are from one experiment representative of three (**a**) independent experiments (mean and s.d. in **a**–**c**, * $P<0.05$, unpaired *t*-test in **b**, abbreviations: Rest, resting; Act, activated; UT, untreated).

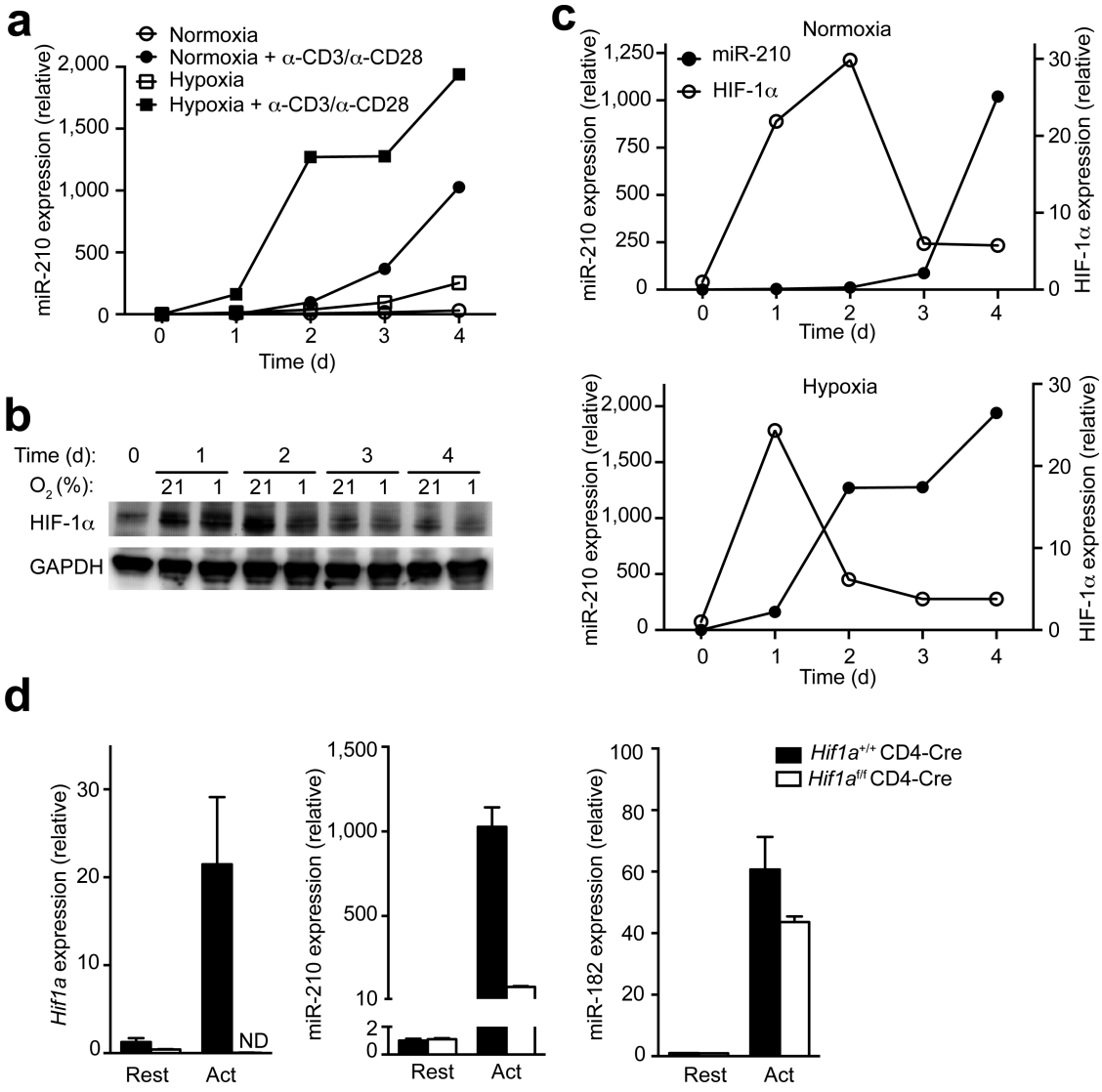

Figure 3. HIF-1α is required for *Mir210* induction

(**a**) Quantitative RT-PCR analysis of miR-210 abundance in unstimulated or anti-CD3– anti-CD28 stimulated $CD4^+$ T cells. Cells were induced for a period of 4 d under normoxic (21% O_2) or hypoxic (1% O_2) conditions and RNA was harvested at the indicated time points. Relative miR-210 expression is normalized to its expression in naive T cells. (**b**) Immunoblot analysis with a HIF-1α-specific or GAPDH-specific antibody in total protein lysates of unstimulated or anti-CD3–anti-CD28 stimulated $CD4^+$ T cells. Cells were induced for a period of 4 d under normoxic (21% O_2) or hypoxic (1% O_2) conditions and protein was harvested at the indicated time points. (**c**) Densitometric analysis of HIF-1α protein levels shown in (**b**) in comparison to miR-210 expression levels presented in (**a**). (**d**) Quantitative RT-PCR analysis of *Hif1a*, miR-210, and miR-182 transcripts in resting or stimulated wild-type (*Hif1a*$^{+/+}$CD4-cre) or HIF-1α–deficient (*Hif1a*$^{f/f}$CD4-cre) $CD4^+$ T cells. Relative expression is normalized to β*2* (*Hif1a*) or sno202 (miR-210 and miR-182) and n=3 independent biological replicates per data point. Data are from one experiment

representative of three (**a**–**c**) independent experiments. (mean and s.d. in a,c,d; abbreviations: Rest, resting; Act, activated; ND not detectable).

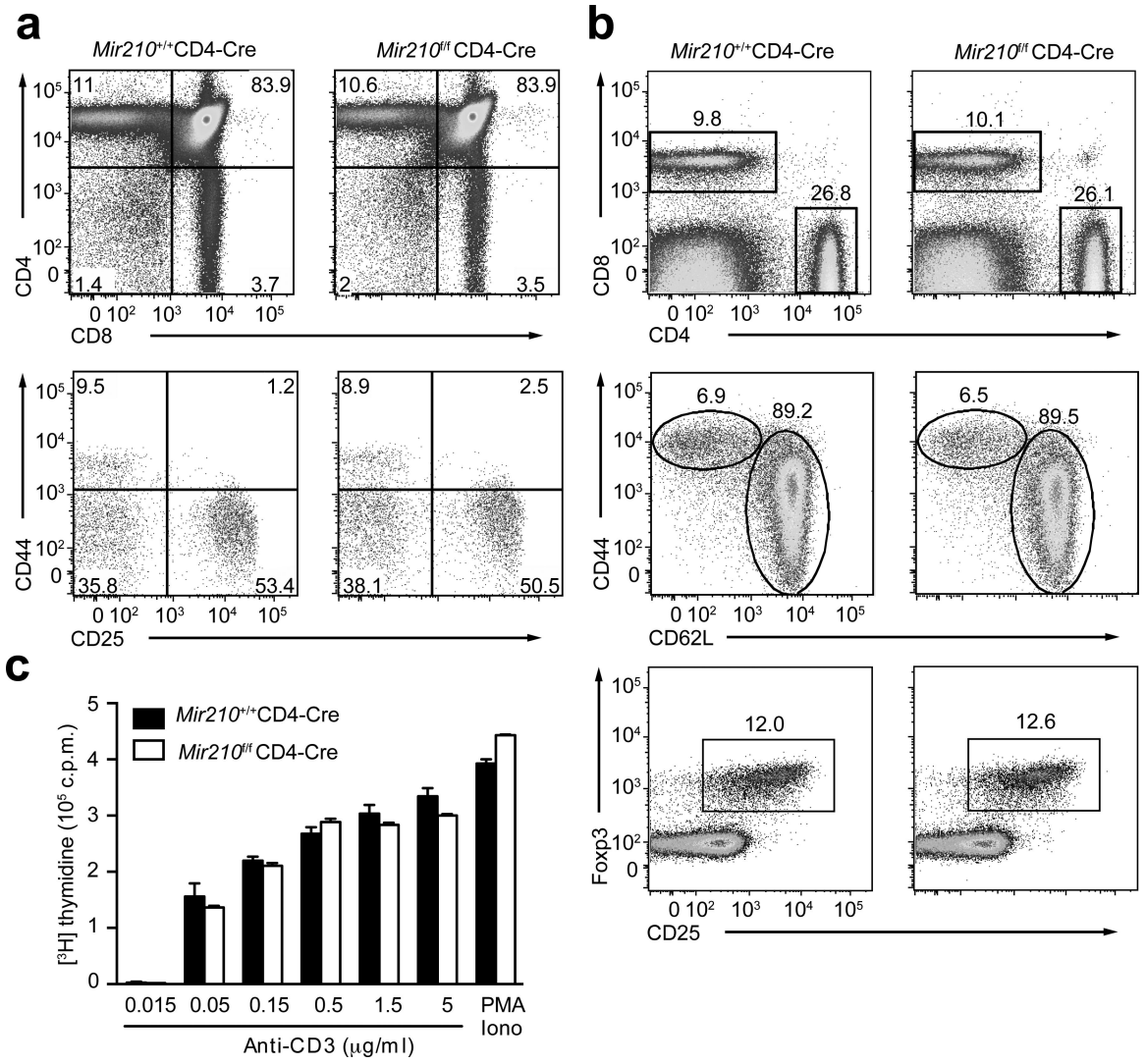

Figure 4. miR-210–deficiency has no apparent effect on T cell development and proliferation

(**a**) Flow cytometry analysis of thymocytes (top panels) or gated double negative thymocytes (bottom panels) from 7 weeks old wild-type or *Mir210*$^{-/-}$ mice, stained with anti-CD4 and anti-CD8 or anti-CD44 and anti-CD25. Numbers adjacent to (or in) outlined areas indicate percent cells in each throughout. (**b**) The surface expression of CD4, CD8 (top), CD44, CD62L (middle) or CD25 and the intracellular expression of Foxp3 (bottom) in splenocytes derived from 7 weeks old wild-type or *Mir210*$^{-/-}$ mice were assessed by flow cytometry. (**c**) T cell proliferation was analyzed in triplicate samples by ^{3}H-thymidine uptake 72 h after stimulation with either anti-CD3 or PMA plus ionomycin (mean and s.d.). Data are representative of three (**a**–**c**) independent experiments.

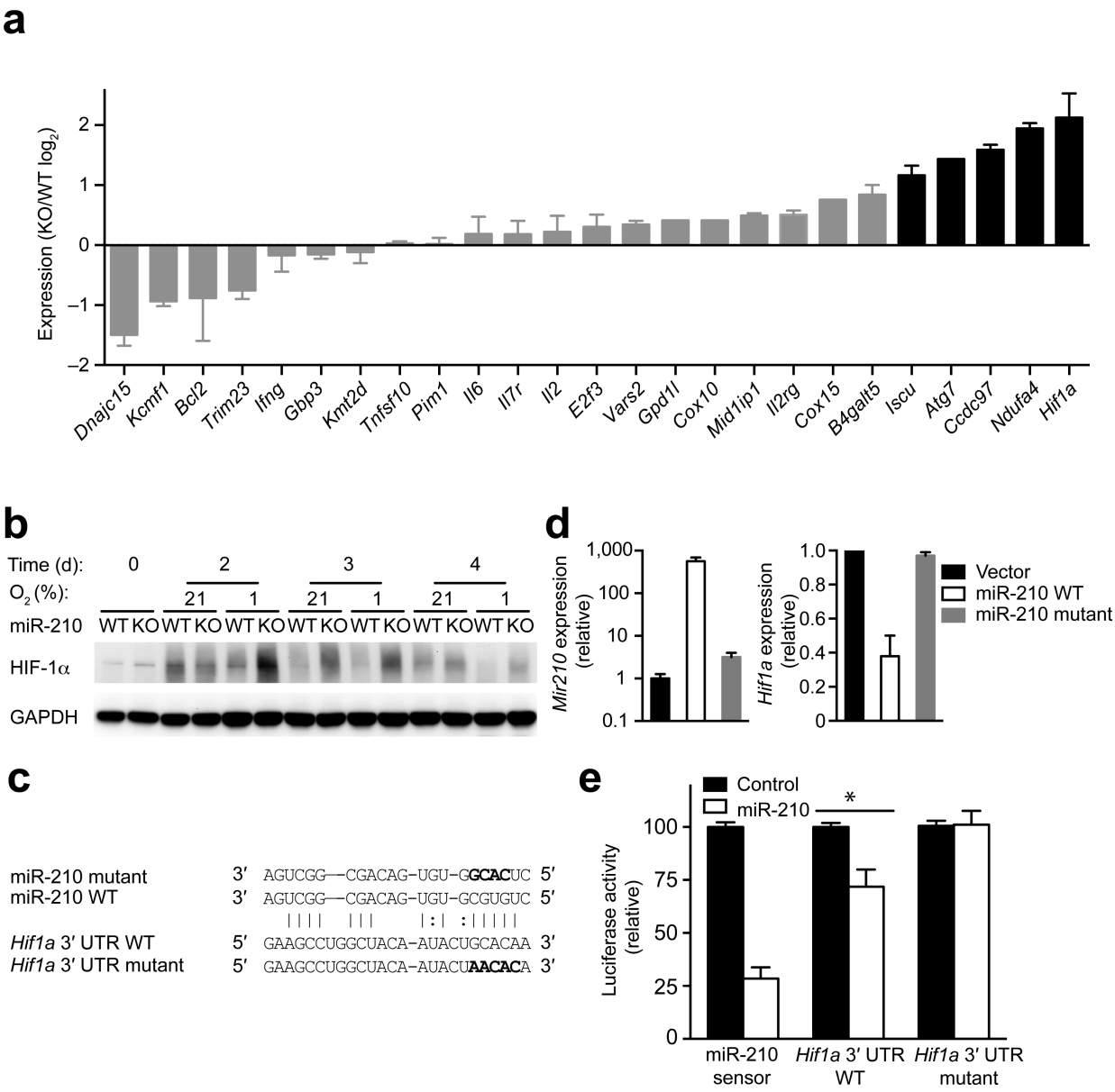

Figure 5. miR-210 directly targets *Hif1a*

(**a**) RT-PCR analysis of the expression of predicted miR-210 target and control gene transcripts in anti-CD3–anti-CD28–stimulated wild-type or *Mir210*$^{-/-}$ CD4^{+} T cells. The genes with more than 2-fold upregulation were highlighted. (**b**) Naive CD4^{+} T cells from wild-type (WT) or *Mir210*$^{-/-}$ (KO) mice were activated by anti-CD3–anti-CD28 under normoxic (21% O_2) or hypoxic (1% O_2) conditions for 4 d and HIF-1α as well as GAPDH protein abundance was detected by immunoblot analysis. (**c**) Sequence alignment between miR-210 and the 3′ UTR of *Hif1a*. The mutated sequences in seed regions of miR-210 and *Hif1a* are highlighted in bold figures. (**d**) *Mir210*$^{-/-}$ CD4^{+} T cells were anti-CD3 plus anti-CD28 stimulated for 36 h, transduced with bicistronic retroviruses expressing GFP (Vector), GFP and wild-type pri-miR-210 (miR-210 WT) or GFP and mutated pri-miR-210 (miR-210 mutant) followed by RT-PCR analysis for *Hif1a* and miR-210 expression in GFP^{+}, CD4^{+} T

cells at 84 h. (**e**) *Mir210*$^{-/-}$ CD4^{+} T cells were cotransfected with luciferase reporters and miR-210 or control miRNA mimics. Luciferase activity was measured 24 h after transfection and was normalized to control transfected cells. (* $P<0.05$, n=4 independent biological replicates per data point *t*-test). Data are from one experiment representative of two (**a**,**b**) or three (**d**) independent experiments. (mean and s.d. in **a**,**d**,**e**).

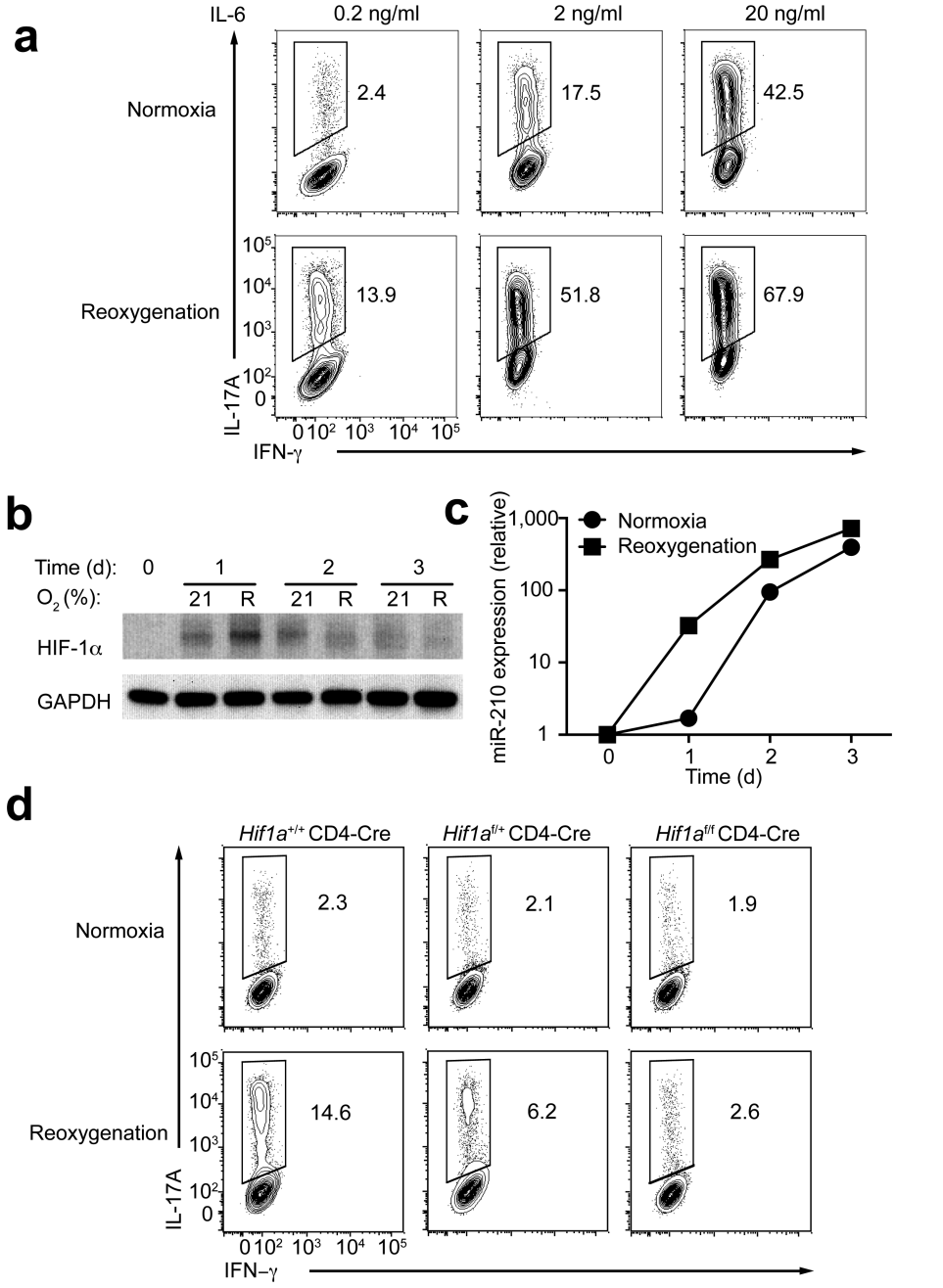

Figure 6. Priming of naive T cells under reoxygenation increases miR-210 abundance

(**a**) Naive $CD4^+$ T cells were polarized towards T_H17 cells with titrated doses of IL-6 under normoxic or reoxygenation conditions (**Supplementary Fig. 6a**), followed by intracellular staining of IL-17A and IFN-γ. (**b–c**) Immunoblot analysis of HIF-1α and GAPDH and RT-PCR analysis of miR-210 in T_H17 cells polarized under normoxic or reoxygenation conditions (0.2 ng/ml of IL-6). Relative miR-210 abundance was normalized to its expression in naive T cells. (**d**) Naive $CD4^+$ T cells from *Hif1a*$^{+/+}$CD4-Cre, *Hif1a* $^{f/+}$CD4-Cre or *Hif1a*$^{f/f}$CD4-Cre mice were differentiated under T_H17 skewing conditions with 0.2 ng/ml of IL-6 under normoxic or reoxygenation conditions, followed by intracellular

staining of IL-17A and IFN-γ. Data are representative of two (**b**,**c**,**d**) or three (**a**) independent experiments. (mean and s.d. in **c**).

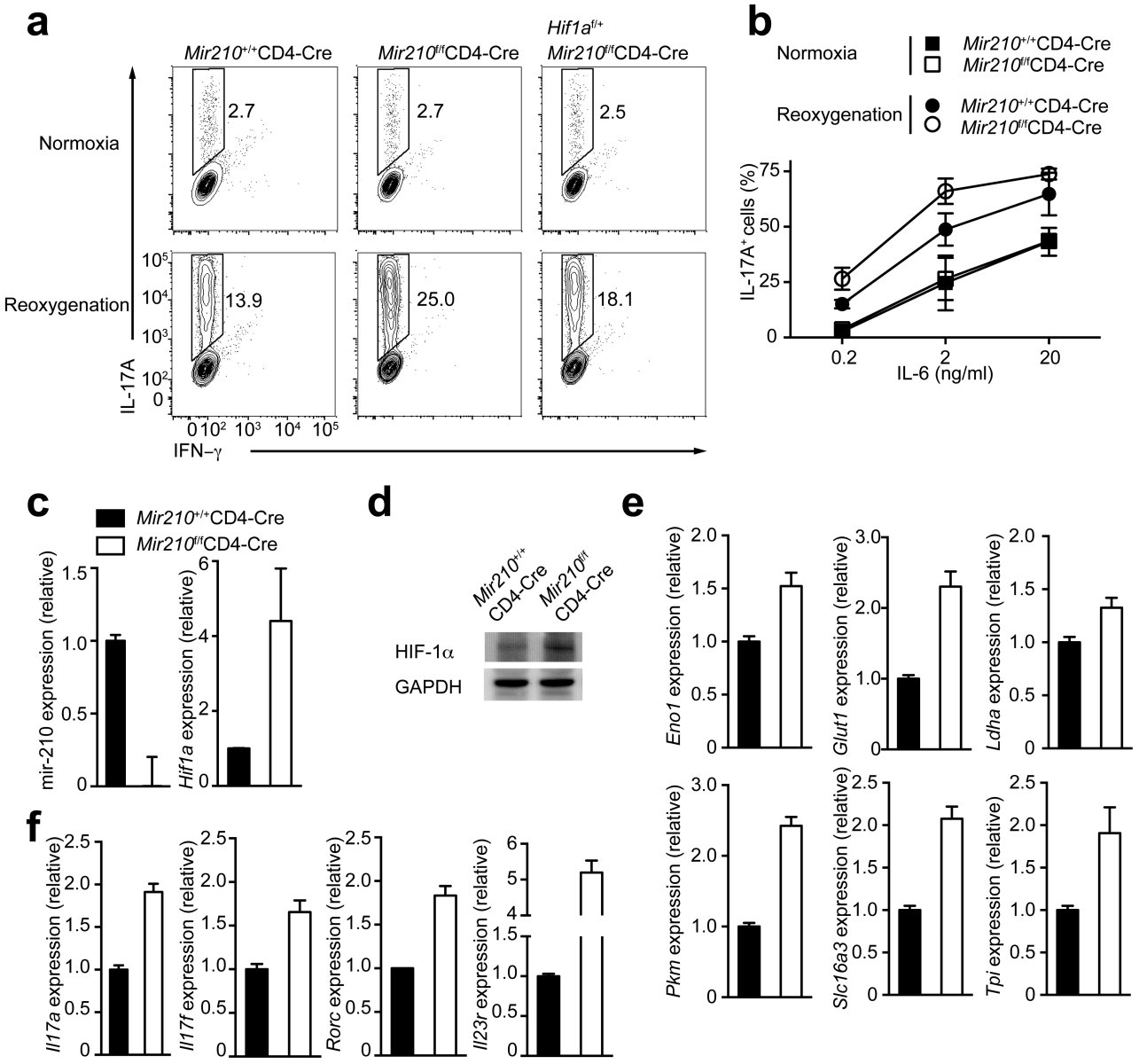

Figure 7. miR-210–deficiency along with reoxygenation conditions markedly increases T_H17 differentiation

(**a**) Naive $CD4^+$ T cells from wild-type (*Mir210*$^{+/+}$CD4-Cre), *Mir210*$^{-/-}$ (*Mir210*$^{f/f}$CD4-Cre) or *Hif1a*$^{f/+}$*Mir210*$^{f/f}$CD4-Cre mice were differentiated under T_H17 skewing conditions (0.2 ng/ml of IL-6), followed by intracellular staining of IL-17A and IFN-γ. (**b**) Naive $CD4^+$ T cells from wild-type (*Mir210*$^{+/+}$CD4-Cre) or *Mir210*$^{-/-}$ (*Mir210*$^{f/f}$CD4-Cre) mice were differentiated under T_H17 skewing conditions with varying doses of IL-6 under normoxic or reoxygenetion conditions, followed by intracellular staining of IL-17A and IFN-γ. (**c–d**) Wild-type or *Mir210*$^{-/-}$ T cells were T_H17 differentiated under reoxygenetion conditions as described in (**a**) for 3 d. Transcripts of miR-210 and *Hif1a* were detected by RT-PCR analysis; HIF-1α and GAPDH protein levels were detected by immunoblot analysis. (**e–f**) Quantitative RT-PCR analysis of HIF-1α target genes of the glycolytic pathway *(Eno1, Glut1, Ldha, Pkm, Slc16a3 and Tpi)* and T_H17 signature genes (*Il17a, Il17f, Rorc* and *Il23r)*

in wild-type or *Mir210*$^{-/-}$ CD4^{+} T_H17 cells that were differentiated under reoxygenetion conditions. Relative expression is normalized to sno202 (miR-210) or β-*2m* (the rest of genes). Data are from one experiment representative of two (**a** right, **d**,**e**), three (**c**,**f**) or four (**a** left and middle, **b**) independent experiments. (mean and s.d. in **b**,**c**,**e**,**f**).

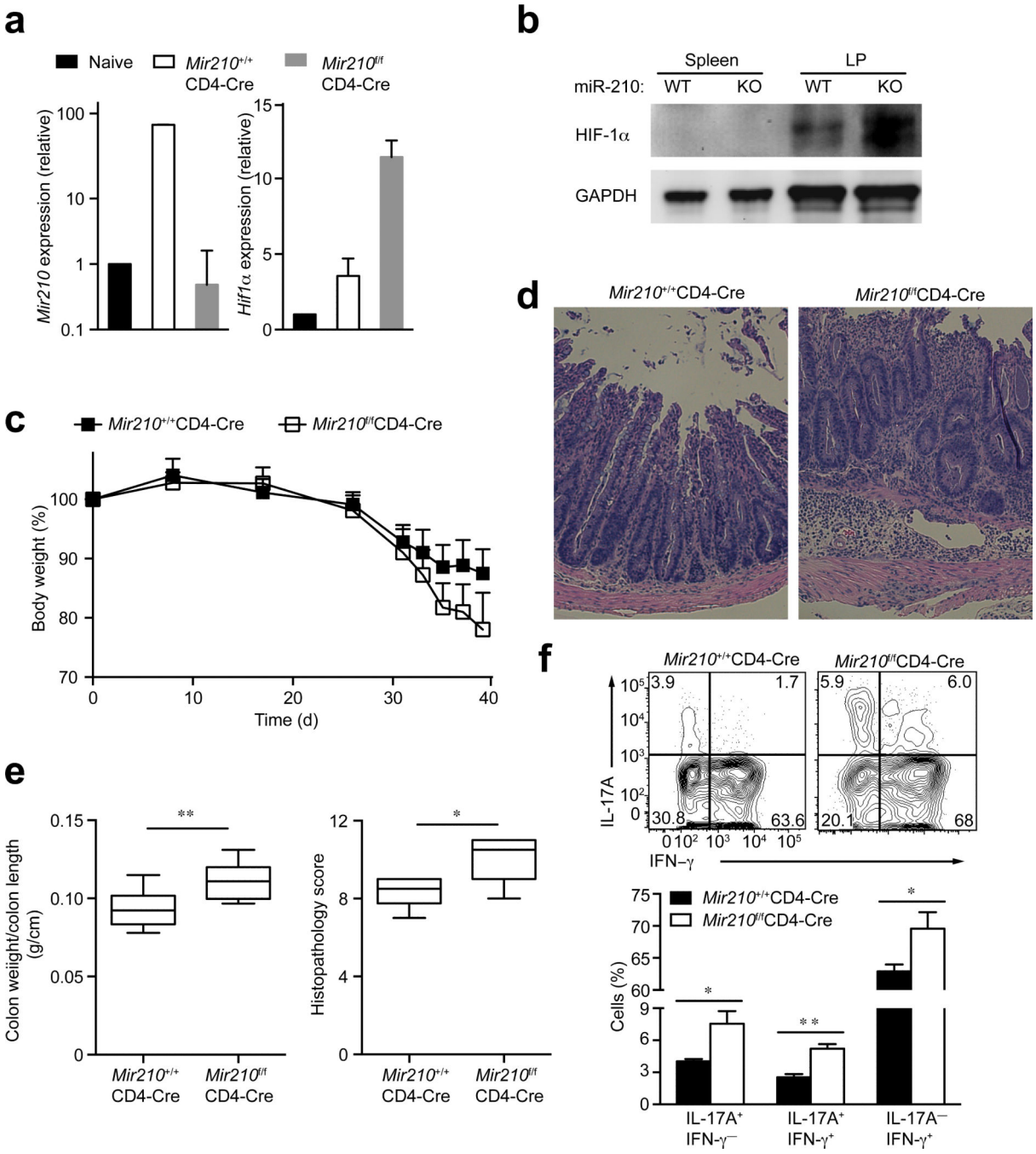

Figure 8. miR-210 in T cells ameliorates IBD disease in a CD4$^+$ T cell transfer model of colitis

(**a**) Wild-type (*Mir210*$^{+/+}$CD4-Cre) or *Mir210*$^{-/-}$ (*Mir210*$^{f/f}$CD4-Cre) naive T cells were transferred into *Rag2*$^{-/-}$ recipient mice. Five weeks later, the colons from recipient mice were excised and lamina propria CD4$^+$ T cells were isolated from the colon. Naive CD4$^+$ T cells were included as a control. miR-210 abundance and *Hif1a* transcripts were analyzed by RT-PCR analysis. (**b**) HIF-1α as well as GAPDH protein abundance in CD4$^+$ T cells isolated from spleen or lamina propria of *Rag2*$^{-/-}$ recipient mice described in (**a**) was detected by immunoblot analysis. (**c**) Change in body weight of *Rag2*$^{-/-}$ recipient mice

given wild-type or *Mir210*$^{-/-}$ naive T cells (n=9 per group). (**d**) Histopathology of distal colon at 5.5 weeks after transfer. Original magnification, X100. (**e**) Ratio of colon weight vs colon length (n=8–9 per group) and histopathological score (n=6–8 per group) of each group are shown. (**f**) Expression of IL-17A and IFN-γ in CD4^{+} T cells isolated from lamina propria (n=3–4 mice per group). * $P<0.05$, ** $P<0.001$, unpaired *t*-test. Data are from one experiment representative of two (**a**–**f**) independent experiments.